

Trajectory equations of interaction and evolution behaviors of a novel multi-soliton to a (2+1)-dimensional shallow water wave model

Xi-Yu Tan(谭茜宇) and Wei Tan(谭伟)

Citation: Chin. Phys. B, 2025, 34 (**4**): 040202. DOI: 10.1088/1674-1056/ada7da
Journal homepage: http://cpb.iphy.ac.cn; http://iopscience.iop.org/cpb

What follows is a list of articles you may be interested in

Trajectory equation of a lump before and after collision with other waves for generalized Hirota-Satsuma-Ito equation

Yarong Xia(夏亚荣), Kaikai Zhang(张开开), Ruoxia Yao(姚若侠), and Yali Shen(申亚丽)
Chin. Phys. B, 2023, 32 (**10**): 100201. DOI: 10.1088/1674-1056/acd62c

Interaction solutions and localized waves to the (2+1)-dimensional Hirota-Satsuma-Ito equation with variable coefficient

Xinying Yan(闫鑫颖), Jinzhou Liu(刘锦洲), and Xiangpeng Xin(辛祥鹏)
Chin. Phys. B, 2023, 32 (**7**): 070201. DOI: 10.1088/1674-1056/acb9f2

Positon and hybrid solutions for the (2+1)-dimensional complex modified Korteweg-de Vries equations

Feng Yuan(袁丰) and Behzad Ghanbari
Chin. Phys. B, 2023, 32 (**4**): 040201. DOI: 10.1088/1674-1056/ac935b

Trajectory equation of a lump before and after collision with line, lump, and breather waves for (2+1)-dimensional Kadomtsev-Petviashvili equation

Zhao Zhang(张钊), Xiangyu Yang(杨翔宇), Wentao Li(李文涛), Biao Li(李彪)
Chin. Phys. B, 2019, 28 (**11**): 110201. DOI: 10.1088/1674-1056/ab44a3

Painlevé integrability of the supersymmetric Ito equation

Feng-Jie Cen(岑锋杰), Yan-Dan Zhao(赵燕丹), Shuang-Yun Fang(房霜韵), Huan Meng(孟欢), Jun Yu(俞军)
Chin. Phys. B, 2019, 28 (**9**): 090201. DOI: 10.1088/1674-1056/ab38a7

Trajectory equations of interaction and evolution behaviors of a novel multi-soliton to a (2+1)-dimensional shallow water wave model

Xi-Yu Tan(谭茜宇) and Wei Tan(谭伟)†

College of Mathematics and Statistics, Jishou University, Jishou 416000, *China*

(Received 10 October 2024; revised manuscript received 6 January 2025; accepted manuscript online 9 January 2025)

Based on a new bilinear equation, we investigated some new dynamic behaviors of the (2+1)-dimensional shallow water wave model, such as hybridization behavior between different solitons, trajectory equations for lump collisions, and evolution behavior of multi-breathers. Firstly, the N-soliton solution of Ito equation is studied, and some high-order breather waves can be obtained from the N-soliton solutions through paired-complexification of parameters. Secondly, the high-order lump solutions and the hybrid solutions are obtained by employing the long-wave limit method, and the motion velocity and trajectory equations of high-order lump waves are analyzed. Moreover, based on the trajectory equations of the higher-order lump solutions, we give and prove the trajectory theorem of 1-lump before and after interaction with n-soliton. Finally, we obtain some new lump solutions from the multi-solitons by constructing a new test function and using the parameter limit method. Meanwhile, some evolutionary behaviors of the obtained solutions are shown through a large number of three-dimensional graphs with different and appropriate parameters.

Keywords: Ito equation, trajectory equation, multi-solitons, dynamic behavior

PACS: 02.30.Jr, 05.45.Yv, 02.30.Ik

DOI: 10.1088/1674-1056/ada7da **CSTR:** 32038.14.CPB.ada7da

1. Introduction

Solitons, fractals and chaos have been the three most concerning research directions in nonlinear science, related to cosmology, fluid physics, fiber optics, atmospheric science, oceanography, etc.[1] The soliton theory is considered one of the important theories driving the development of nonlinear science, playing a very important role in various fields of natural science.[2,3] It has been widely applied in nonlinear optics, fluid mechanics, plasma physics, condensed matter physics, and other fields. The soliton solution is a special wave solution, which has the characteristic of keeping the shape unchanged during the propagation process, and is widely present in various physical phenomena. The study of soliton solutions and their properties for nonlinear partial differential equations (NPDE) has always been widely studied in the field of nonlinearity. With the introduction and expansion of scattering inversion method,[4] Hirota bilinear method,[5,6] Darboux transform method,[7,8] Riemann–Hilbert approach[9,10] and so on. Some new soliton solutions and structural properties have been discovered, such as lump solution, breather soliton, multi-soliton, rogue wave, etc.[11–16] In recent years, the soliton solutions of NPDE such as shallow water wave equation and KP equation, as well as their applications in fluid dynamics and fiber optic communication, have attracted widespread attention from researchers. Therefore, it is very important to study new soliton solutions and their structural properties of nonlinear equations, among which the interaction or hybrid behavior between different solitons has become one of the key research topics.

Very recently, the study of interaction behavior between different solitons, such as between lump solutions and solitons, between rogue waves and solitons, between lump solutions and breathers, has become a hot topic because of their application value and extensive theory in the field of nonlinear natural science. However, there is little research on the dynamic properties of different soliton interactions before and after, such as trajectory equations, motion velocity, interaction deformation, and evolutionary behavior.[17,18] This article focuses on the study of the evolution behavior of a novel multi-solitons and the trajectory problem of lump interaction for the (2+1)-dimensional shallow water wave model

$$\begin{aligned} &u_{tt}+u_{xxxt}+3\left(uu_{xt}+2u_xu_t\right)\\ &+3u_{xx}\int_{-\infty}^{x}u_t\,\mathrm{d}x'+\alpha u_{yt}+\beta u_{xt}=0, \end{aligned} \tag{1}$$

where α and β denote two arbitrary constants. In 1980, Ito established the well-known (1+1)-dimensional and (2+1)-dimensional Ito equation by generalization of the bilinear KdV equation,[19] therefore, model (1) is often referred to as the Ito equation. Equation (1) is simplified to the (1+1)-dimensional form when $\alpha=0$, $\beta=0$. The introduction of the (2+1)-dimensional Ito equation provides a powerful mathematical tool for the study of the behavior of solitons in multi-dimensional space. As a typical (2+1)-dimensional

†Corresponding author. E-mail: tanwei1008@126.com

© 2025 Chinese Physical Society and IOP Publishing Ltd. All rights, including for text and data mining, AI training, and similar technologies, are reserved.

NPDE, many scholars have studied different forms of soliton solutions for Eq. (1) using different methods. For example, Adem investigated its multiple wave solutions by using multiple exp-function algorithm.[20] Zhang *et al*. studied its high-order localized waves by employing the Hirota derivative operator.[21] Wang *et al*. discussed its dynamics of the rogue waves and solitary waves by applying homoclinic breather limit method.[22] Tan investigated its double breathers and lump–N-solitons via employing Hirota bilinear method.[23] Tian *et al*. obtained its rogue waves and new multi-wave solutions by using three-soliton limit method.[24] The lump solution and the interaction phenomenon related to the lump (or lump-type) solution of Eq. (1) have been studied,[25–32] respectively. However, to the best of authors' knowledge, the evolution behavior of multiple solitons, trajectory problems after interactions between different solitons and high-order breathers of (2+1)-dimensional Ito equation have not been discussed and studied.

The framework of this paper is as follows. In Section 2, we find the N-soliton solutions of the Ito equation, and then obtain the high-order breather solutions, high-order rational solution, M-order lump solutions and the hybrid solutions from the N-soliton solutions by using the paired-complexification of parameters and the long-wave limit method. Furthermore, the trajectory equations of the M-order lump solutions and the hybridization behavior between 1-lump and n-soliton are analyzed. In Section 3, the degradation of a novel multi-solitons and the emergence of a new lump solution will be studied by utilizing parameter limit method.[33] Section 4 summarizes the findings of this paper.

2. Bilinearization and evolution behavior of N-solitons

In this section, we first obtain a new bilinear equation for Eq. (1) through function transformation. Secondly, based on this new bilinear equation, we will investigate the evolution behavior of N-soliton solutions of the (2+1)-dimensional Ito Eq. (1) by using the long-wave limit method, which includes M-order breather wave, M-order lump solution, high-order hybrid solution and the trajectory problem of lump solutions before and after interaction with different solitons.

To eliminate the integral sign in Eq. (1), we can rewrite Eq. (1) as

$$\begin{cases} u_t = v_x, \\ v_t + \alpha v_y + \beta v_x + 3(uv)_x + v_{xxx} = 0, \end{cases} \tag{2}$$

which is called equivalent coupled system. Further more, we take the following transformation:

$$\begin{cases} u(x,y,t) = 2(\ln f)_{xx}, \\ v(x,y,t) = u_0 + 2(\ln f)_{xt}, \end{cases} \tag{3}$$

where u_0 is a real constant and f is a test function to be selected later. Substituting Eq. (3) into Eq. (2), system (2) can be converted to the following bilinear form, which is quite different from the work in Ref. [23–30]:

$$\begin{aligned} &P(D_x, D_y, D_t) f \cdot f \\ &= (D_x^3 D_t + \alpha D_y D_t + \beta D_x D_t + 3u_0 D_x^2 + D_t^2) f \cdot f = 0, \end{aligned} \tag{4}$$

while the symbol D_- stands for Hirota derivative. In Refs. [17, 34], the authors studied the generalized Hirota–Satsuma–Ito equation (gHSI) by using the long-wave limit method. In fact, the bilinear equation (4) and the bilinear forms of gHSI are different and cannot be derived from each other. In this article, we will further investigate the topic of Refs. [17,34] by studying the Ito equation (1).

2.1. The N-soliton solutions

In order to obtain the N-soliton solutions of Ito Eq. (2), suppose the test function f can be represented by the following form, on the basis of bilinear equation (4), we have

$$f = f_N = \sum_{\mu=0,1} \exp\left(\sum_{i=1}^{N} \mu_i \zeta_i + \sum_{i<j}^{(N)} A_{ij} \mu_i \mu_j \right), \tag{5}$$

where $\sum_{\mu=0,1}$ denotes the summation of all the cases of $\mu_i = 0$ or 1 when $1 \le i \le N$, and $\sum_{i<j}^{(N)}$ represents the summation of all the cases of (i, j) that satisfy condition $1 \le i < j \le N$. By using Maple software and combining Eqs. (4) and (5), we can obtain the following parameter relationships:

$$\begin{cases} \zeta_i = k_i(m_i x + p_i y + q_i t) + \gamma_i, \\ p_i = -\dfrac{k_i^2 m_i^3 q_i + \beta m_i q_i + 3u_0 m_i^2 + q_i^2}{\alpha q_i}, \\ e^{A_{12}} = \dfrac{m_i m_j q_i q_j (k_i q_i - k_j q_j)(k_i m_i - k_j m_j) - u_0 (m_i q_j - m_j q_i)^2}{m_i m_j q_i q_j (k_i q_i + k_j q_j)(k_i m_i + k_j m_j) - u_0 (m_i q_j - m_j q_i)^2}, \end{cases} \tag{6}$$

where $q_i \neq 0$ and k_i, m_i, γ_i are arbitrary parameters. By substituting Eqs. (5) and (6) into Eq. (3), we can get the N-soliton solutions of Ito Eq. (1) (see Fig. 1).

By providing the spatial structure diagrams of solitons 1, 2 and 3, we can clearly observe the evolution behavior of multi-soliton solutions as the number of solitons increases. The parameter values of (a) are $u_0 = 0$, $k_1 = \frac{1}{2}$, $m_1 = 2$, $q_1 = \frac{1}{2}$, $\beta = 2$, $\alpha = 5$, $\gamma_1 = 1$; the parameter values of (b) are $u_0 = 1$, $k_1 = \frac{1}{2}$, $k_2 = \frac{1}{2}$, $m_1 = 1$, $m_2 = -2$, $q_1 = 1$, $q_2 = 2$, $\beta = 1$, $\alpha = 1$, $\gamma_1 = 1$, $\gamma_2 = 1$, and when the parameter values are $u_0 = 1$, $k_1 = 1$, $k_2 = 1$, $k_3 = \frac{3}{2}$, $m_1 = 1$, $m_2 = -1$, $m_3 = 1$, $q_1 = 1$, $q_2 = 1$, $q_3 = -1$, $\beta = 2$, $\alpha = 1$, $\gamma_1 = 1$, $\gamma_2 = 1$, $\gamma_3 = 1$, we can get (c).

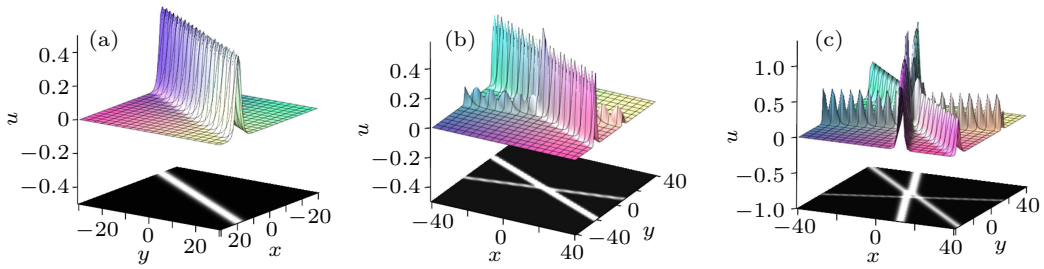


Fig. 1. The spatial structure plots of N-solitons at $t = 0$: (a) $N = 1$; (b) $N = 2$; (c) $N = 3$.

2.2. The M-order breather waves

Based on the N-soliton solution Eqs. (5) and (6), we investigate the M-order breather wave of Ito Eq. (2) by applying parameter paired conjugate mutual transformation techniques. In order to obtain the M-order breather waves of Ito Eq. (1), we take the following parameter relationships:

$$\begin{aligned} &N = 2M, \quad k_{M+j} = k_j^* = k, \quad m_{M+j} = m_j^* = a_j - b_j I, \\ &q_{M+j} = q_j^* = c_j - d_j I, \quad \mathrm{e}^{\gamma_j} = 1, \quad (j = 1,2,\ldots,M), \end{aligned} \tag{7}$$

where the symbol I represents imaginary units and $*$ denotes taking conjugation. We substitute Eqs. (5)–(7) into Eq. (3) to get the M-order breather waves of Ito Eq. (2).

Next, we will take 1-order breather wave as an example to demonstrate the process of finding M-order breather waves. Firstly, in Eq. (5), we take $N = 2$ and obtain the following equation:

$$f_2 = 1 + \mathrm{e}^{\zeta_1} + \mathrm{e}^{\zeta_2} + \mathrm{e}^{\zeta_1+\zeta_2+A_{12}}. \tag{8}$$

Secondly, taking $k_2 = k_1 = k$, $m_2 = m_1^* = a_1 - b_1 I$, $q_2 = q_1^* = c_1 - d_1 I$, $p_2 = p_1^* = e_1 - g_1 I$, $\mathrm{e}^{\gamma_1} = \mathrm{e}^{\gamma_2} = 1$ in Eq. (7) and substituting them into Eq. (8), we get

$$\hat{f}_2 = 2\mathrm{e}^{k\phi_1}(\sqrt{M}\cosh(k\phi_1 + \ln\sqrt{M}) + \cos(k\phi_2)),$$

where

$$\begin{aligned} &\phi_1 = a_1 x + e_1 y + c_1 t, \quad M = \mathrm{e}^{A_{12}}, \\ &\phi_2 = b_1 x + g_1 y + d_1 t, \end{aligned} \tag{9}$$

and the parameters a_1, b_1, c_1, d_1, e_1, f_1 are some undetermined real numbers. Finally, we get the 1-order breather wave by substating $\hat{f}_2$ into transformation (3),

$$\begin{cases} u = \dfrac{2k^2\left(a_1^2 M - b_1^2 + (a_1^2 - b_1^2)\sqrt{M}\cosh(k\phi_1 + \ln\sqrt{M})\cos(k\phi_2) + 2a_1 b_1\sqrt{M}\sinh(k\phi_1 + \ln\sqrt{M})\sin(k\phi_2)\right)}{\left(\sqrt{M}\cosh(k\phi_1 + \ln\sqrt{M}) + \cos(k\phi_2)\right)^2}, \\ v = u_0 + \dfrac{2k^2\left(a_1 c_1 M - b_1 d_1 + (a_1 c_1 - b_1 d_1)\sqrt{M}\cosh(k\phi_1 + \ln\sqrt{M})\cos(k\phi_2) + (a_1 d_1 + b_1 c_1)\sqrt{M}\sinh(k\phi_1 + \ln\sqrt{M})\sin(k\phi_2)\right)}{\left(\sqrt{M}\cosh(k\phi_1 + \ln\sqrt{M}) + \cos(k\phi_2)\right)^2}. \end{cases} \tag{10}$$

In fact, from the expression (10) and spatial structure Fig. 2(a), we can clearly see that the obtained 1-order breather wave (10) is a type of Akhmediev breathers.[35] Similar to the process of finding 1-order breather wave, we take $N = 4$ and 6 in Eqs. (5) and (7) and substitute them into Eq. (3) to obtain 2-order and 3-order breather waves of Ito Eq. (2). Because there are some free parameters in the M-order breather waves, we can get different three-dimensional diagrams of M-order breather waves by selecting different parameters. In Fig. 2, we give the spatiotemporal evolution structure of the M-order breather waves with increasing order M. The parameter values are as follows: (a) $u_0 = -\frac{1}{2}$, $k_1 = k_2 = 1$, $m_1^* = m_2 = -I$, $q_1^* = q_2 = 2 - I$, $\alpha = 1$, $\beta = 1$; (b) $u_0 = -\frac{1}{2}$, $m_1 = m_3^* = 1 + \frac{1}{4}I$, $m_2 = m_4^* = \frac{1}{8} + I$, $q_1 = q_3^* = \frac{1}{12} + I$, $q_2 = q_4^* = 1 + \frac{1}{4}I$, $\alpha = 1$, $\beta = 1$, $k_i = 1$ $(i = 1,2,3,4)$; (c) $u_0 = -\frac{1}{2}$, $m_1 = m_4^* = 1 + \frac{1}{4}I$, $m_2 = m_5^* = \frac{1}{8} + I$, $m_3 = m_6^* = \frac{1}{2} + I$, $q_1 = q_4^* = \frac{1}{12} + I$, $q_2 = q_5^* = 1 + \frac{1}{4}I$, $q_3 = q_6^* = 1 + \frac{1}{10}I$, $\alpha = 1$, $\beta = 1$, $k_i = \frac{1}{2}$, $(i = 1,2,\ldots,6)$.

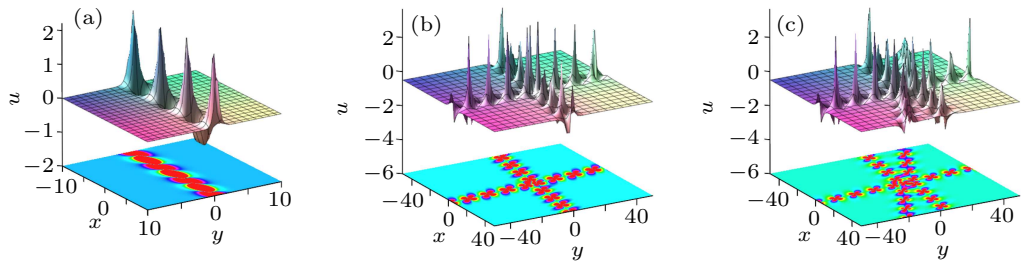


Fig. 2. The spatial structure plots of M-order breather soliton at $t = 0$: (a) $M = 1$, (b) $M = 2$, (c) $M = 3$.

2.3. The M-lump solutions and trajectory equations

The purpose of this subsection is to construct the M-lump solutions for the (2+1)-dimensional Ito Eq. (1). Firstly, we get the rational solutions by the long-wave limit method, and then get the M-lump solutions from the rational solutions by the paired-complexification of parameters. In order to get the M-lump solutions of Ito Eq. (1), we set $\gamma_i = \mathrm{I}\pi$ in Eqs. (5) and (6), then f_N can be expressed by the following form:

$$f_N = \sum_{\mu=0,1} \prod_{i=1}^{N} (-1)^{\mu_i} \exp(\mu_i \xi_i) \prod_{i<j}^{(N)} \exp(\mu_i \mu_j A_{ij}), \tag{11}$$

with $\xi_i = k_i(m_i x - \frac{k_i^2 m_i^3 q_i + \beta m_i q_i + 3u_0 m_i^2 + q_i^2}{\alpha q_i} y + q_i t)$. Based on the long-wave limit method, we take $k_i/k_j = O(1)$ and let k_i tend to 0 in Eqs. (11) and (5). As a result, we can get

$$\begin{aligned} f_N = & \sum_{\mu=0,1} \prod_{i=1}^{N} (-1)^{\mu_i} (1 + \mu_i k_i \theta_i) \\ & \times \prod_{i<j}^{(N)} \exp(1 + \mu_i \mu_j k_i k_j \Lambda_{ij}) + O(k^{N+1}), \end{aligned} \tag{12}$$

where

$$\begin{cases} \theta_i = m_i x - \dfrac{\beta m_i q_i + 3u_0 m_i^2 + q_i^2}{\alpha q_i} y + q_i t, \\ \exp(A_{ij}) \overset{\text{def}}{=} 1 + \Lambda_{ij}, \\ \Lambda_{ij} = \dfrac{2 m_i m_j q_i q_j (m_i q_j + m_j q_i)}{u_0 (m_i q_j - m_j q_i)^2}. \end{cases} \tag{13}$$

Since u and v are given by transformation (3), when f_N is multiplied by a constant, we can reduce it to the following rational solutions:

$$\begin{aligned} f_N = & \prod_{i=1}^{N} \theta_i + \frac{1}{2} \sum_{i,j}^{(N)} \Lambda_{ij} \prod_{r \neq i,j}^{N} \theta_r + \\ & + \frac{1}{2!2^2} \sum_{i,j,p,s}^{(N)} \Lambda_{ij} \Lambda_{ps} \prod_{r \neq i,j,p,s}^{N} \theta_r + \cdots, \\ & + \frac{1}{M! 2^M} \sum_{i,j,\ldots,m,n}^{(N)} \overbrace{\Lambda_{ij} \Lambda_{kl} \ldots, \Lambda_{mn}}^{M} \prod_{s \neq i,j,k,l,\ldots,m,n}^{N} \theta_s + \cdots, \end{aligned} \tag{14}$$

where the symbol $\sum_{i,j,\ldots,m,n}^{(N)}$ represents the same meaning as the previous text. In Eq. (14), we set $N = 1, 2, \ldots$, and substitute them into Eq. (3) to obtain the N-order rational solution of (2+1)-dimensional Ito Eq. (2).

For example, when $N = 2$, we get

$$f_2 = \theta_1 \theta_2 + \Lambda_{12}. \tag{15}$$

Substituting Eqs. (13) and (15) into Eq. (3), we get the 2-order rational solution

$$\begin{cases} u(x,y,t) = \dfrac{2(2m_1 m_2 \Lambda_{12} - m_2^2 \theta_1^2 - m_1^2 \theta_2^2)}{(\theta_1 \theta_2 + \Lambda_{12})^2}, \\ v(x,y,t) = u_0 + \dfrac{2((m_2 q_1 + m_1 q_2)\Lambda_{12} - m_1 q_1 \theta_2^2 - m_2 q_2 \theta_1^2)}{(\theta_1 \theta_2 + \Lambda_{12})^2}. \end{cases}$$

When $N = 3, 4$, we have

$$\begin{aligned} f_3 = & \theta_1 \theta_2 \theta_3 + \Lambda_{12} \theta_3 + \Lambda_{23} \theta_1 + \Lambda_{31} \theta_2, \\ f_4 = & \theta_1 \theta_2 \theta_3 \theta_4 + \Lambda_{12} \theta_3 \theta_4 + \Lambda_{13} \theta_2 \theta_4 \\ & + \Lambda_{14} \theta_2 \theta_3 + \Lambda_{23} \theta_1 \theta_4 + \Lambda_{24} \theta_1 \theta_3 \\ & + \Lambda_{34} \theta_1 \theta_2 + \Lambda_{12} \Lambda_{34} + \Lambda_{13} \Lambda_{24} + \Lambda_{14} \Lambda_{23}. \end{aligned} \tag{16}$$

Similarly, the 3-order and 4-order rational solutions can be obtained by substituting Eqs. (16) and (12) into Eq. (3), respectively. Furthermore, through this calculation method, we can obtain the N-order rational solutions of Ito Eq. (2).

In order to get the M-lump solutions of Ito Eq. (2), we set $N = 2M$ in Eq. (14) and take $m_{M+i} = m_i^* = a_{1i} - b_{1i} I, q_{M+i} = q_i^* = c_{1i} - d_{1i} I$ $(i = 1, 2, \cdots, M)$ in Eq. (13). Take 1-lump solution for example, when $M = 1$, we take $m_2 = m_1^* = a_{11} - b_{11} I, q_2 = q_1^* = c_{11} - d_{11} I$ in Eq. (15), then f_2 can be expressed by the following form:

$$\begin{aligned} \hat{f}_2(x,y,t) = & \left(a_{11} x - \frac{\beta(a_{11} c_{11}^2 + a_{11} d_{11}^2) + 3u_0(a_{11}^2 c_{11} - b_{11}^2 c_{11} + 2a_{11} b_{11} d_{11}) + (c_{11}^3 + c_{11} d_{11}^2)}{\alpha(c_{11}^2 + d_{11}^2)} y + c_{11} t \right)^2 \\ & + \left(b_{11} x - \frac{\beta(b_{11} c_{11}^2 + b_{11} d_{11}^2) + 3u_0(b_{11}^2 d_{11} - a_{11}^2 d_{11} + 2a_{11} b_{11} c_{11}) + (d_{11}^3 + d_{11} c_{11}^2)}{\alpha(c_{11}^2 + d_{11}^2)} y + d_{11} t \right)^2 \\ & + \frac{-(a_{11}^2 + b_{11}^2)(c_{11}^2 + d_{11}^2)(a_{11} c_{11} + b_{11} d_{11})}{u_0 (b_{11} c_{11} - a_{11} d_{11})^2} \\ \overset{\text{def}}{=} & \varsigma_1^2 + \varsigma_2^2 + \Delta. \end{aligned}$$

Substituting $\hat{f}_2(x,y,t)$ into transformation (3), we can obtain the following 1-lump solution (see Fig. 3(a)):

$$\begin{cases} u(x,y,t) = 4 \dfrac{(b_{11}^2 - a_{11}^2)(\varsigma_1^2 - \varsigma_2^2) - 4a_{11} b_{11} \varsigma_1 \varsigma_2 + (a_{11}^2 + b_{11}^2)\Delta}{(\varsigma_1^2 + \varsigma_2^2 + \Delta)^2}, \\ v(x,y,t) = u_0 + 4 \dfrac{(b_{11} d_{11} - a_{11} c_{11})(\varsigma_1^2 - \varsigma_2^2) - 2(a_{11} d_{11} + b_{11} c_{11}) \varsigma_1 \varsigma_2 + (a_{11} c_{11} + b_{11} d_{11})\Delta}{(\varsigma_1^2 + \varsigma_2^2 + \Delta)^2}. \end{cases} \tag{17}$$

Similar to the process of getting 1-lump solution, when $N=4$, $M=2$, taking $m_3=m_1^*=a_{11}-b_{11}I$, $m_4=m_2^*=a_{12}-b_{12}I$, $q_3=q_1^*=c_{11}-d_{11}I$, $q_4=q_2^*=c_{12}-d_{12}I$ into Eq. (14), we can get the 2-lump solutions (see Fig. 3(b)). When $N=6$, $M=3$, choosing $m_4=m_1^*=a_{11}-b_{11}I$, $m_5=m_2^*=a_{12}-b_{12}I$, $m_6=m_3^*=a_{13}-b_{13}I$, $q_4=q_1^*=c_{11}-d_{11}I$, $q_5=q_2^*=c_{12}-d_{12}I$, $q_6=q_3^*=c_{13}-d_{13}I$ in Eq. (14), we can get the 3-lump solutions (see Fig. 4(c)). Moreover, when $N=2M$, choosing $m_{M+i}=m_i^*=a_{1i}-b_{1i}I$, $q_{M+i}=q_i^*=c_{1i}-d_{1i}I$ $(i=1,2,\ldots,M)$ in Eq. (14), we can get the M-lump solutions of Ito Eq. (2). We provide some three-dimensional diagrams of the 1, 2 and 3-lump solutions to demonstrate the evolutionary behavior of the M-lump solutions. When $u_0=\frac{1}{2}$, $a_{11}=1$, $b_{11}=\frac{1}{2}$, $c_{11}=-2$, $d_{11}=1$, $\alpha=2$, $\beta=1$, the spatial structure diagram (a) of 1-lump can be obtained. And when $u_0=-\frac{1}{2}$, $a_{11}=-\frac{3}{4}$, $b_{11}=\frac{1}{10}$, $a_{12}=-\frac{3}{5}$, $b_{12}=\frac{1}{4}$, $c_{11}=-\frac{2}{5}$, $d_{11}=\frac{5}{2}$, $c_{12}=-\frac{1}{5}$, $d_{12}=\frac{6}{5}$, $\alpha=2$, $\beta=\frac{1}{2}$, we can obtain the spatial structure diagram of 2-lump. Of course, the spatial structure diagram of 3-lump can be obtained when the values of parameters are $u_0=\frac{1}{2}$, $a_{11}=-\frac{3}{5}$, $b_{11}=\frac{1}{5}$, $a_{12}=-\frac{3}{5}$, $b_{12}=\frac{2}{5}$, $a_{13}=\frac{3}{4}$, $b_{13}=\frac{1}{4}$, $c_{11}=\frac{1}{4}$, $d_{11}=\frac{2}{5}$, $c_{12}=-\frac{1}{4}$, $d_{12}=-\frac{1}{2}$, $c_{13}=\frac{1}{4}$, $d_{13}=-2$, $\alpha=2$, $\beta=1$. From the above three-dimensional diagrams, we can clearly see that with the increase of order M, the number of peaks in the lump solutions is also increasing.

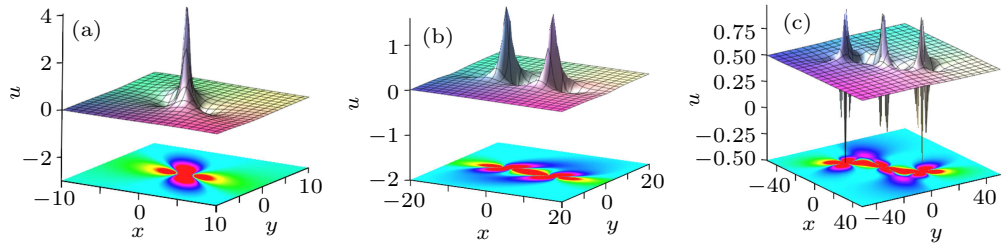


Fig. 3. The spatial structure plots of M-lump solution at $t=0$: (a) $M=1$; (b) $M=2$; (c) $M=3$.

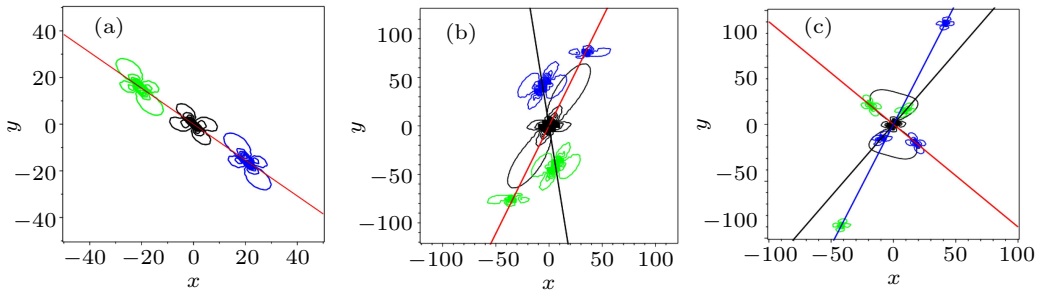


Fig. 4. The trajectory plots of M-lump at $t=-40$ (green), 0 (black), 40 (blue): (a) the trajectory of 1-lump along $y=-\frac{10}{13}x$; (b) the trajectory of 2-lump along $y=\frac{916}{413}x$ (red) and $y=-\frac{320}{47}x$ (black); (c) the trajectory of 3-lump along $y=-\frac{82}{91}x$ (red), $y=\frac{82}{65}x$ (black) and $y=\frac{17}{8}x$ (blue).

For the 1-lump solution $u=2\ln(\theta_1\theta_2+\Lambda_{12})_{xx}$, we can get its peak as follows by solving the equations $u_x=0, u_y=0$ and combining the positive and negative of $u_{xx}, u_{xx}u_{yy}-u_{xy}^2$:

$$\begin{aligned} x&=-\frac{\beta q_1q_2+3u_0(m_1q_2+m_2q_1)}{3u_0m_1m_2-q_1q_2}t,\\ y&=-\frac{\alpha q_1q_2}{3u_0m_1m_2-q_1q_2}t. \end{aligned} \tag{18}$$

The movement trajectory and speed[17,36] of 1-lump solution are shown as follows:

$$\begin{aligned} y&=\frac{\alpha q_1q_2}{\beta q_1q_2+3u_0(m_1q_2+m_2q_1)}x,\\ v&=\sqrt{\frac{(\beta q_1q_2+3u_0(m_1q_2+m_2q_1))^2}{(3u_0m_1m_2-q_1q_2)^2}+\frac{\alpha^2q_1^2q_2^2}{(3u_0m_1m_2-q_1q_2)^2}}. \end{aligned} \tag{19}$$

For 2-lump and 3-lump, before and after the interaction, their trajectory equations are consistent with Eq. (18) of 1-lump, which does not change with the increase of order, so it will not be explained here. When the parameters are $u_0=-\frac{1}{4}$, $\alpha=2$, $\beta=1$, $m_1^*=m_2=-\frac{1}{4}-\frac{1}{10}I$, $q_1^*=q_2=-\frac{2}{5}-3I$, $m_3^*=m_4=-\frac{6}{5}-\frac{3}{4}I$, $q_3^*=q_4=\frac{6}{5}+\frac{3}{4}I$, we obtain the trajectory diagram of 2-lump, and calculate that the movement trajectories of its peaks are $y=\frac{916}{413}x$ and $y=-\frac{320}{47}x$. In Fig. 4, by selecting $u_0=\frac{1}{2}$, $\alpha=2$, $\beta=1$, $m_1^*=m_2=-\frac{3}{5}-\frac{1}{5}I$, $q_1^*=q_2=\frac{1}{4}-\frac{1}{5}I$, $m_3^*=m_4=-\frac{3}{5}-\frac{2}{5}I$, $q_3^*=q_4=-\frac{1}{5}+\frac{1}{4}I$, $m_5^*=m_6=\frac{3}{4}-\frac{1}{4}I$, $q_5^*=q_6=\frac{3}{4}+3I$, we get the trajectory diagram of 3-lump.

2.4. Hybridization behavior and trajectory equations

In this subsection, we will investigate the hybridization behavior of Ito Eq. (2) which is made up of solitons, breather waves and lump solutions by using the long-wave limit method and paired-complexification of parameters. And we mainly study the hybridization behavior composed of 1-lump solution and n-solitons, and the hybridization behavior composed of 1-order breather wave and n-solitons $(n=1,2)$. The hybridization behavior of Ito Eq. (2) can be studied by taking

some special parameters in Eqs. (5) and (6). To study the hybridization behavior and trajectory equations of 1-lump before and after interaction with different forms of n-solitons, we first take the following relationship equation:

$$m_2 = m_1^* = a_{11} - b_{11} I, \quad q_2 = q_1^* = c_{11} - d_{11} I. \tag{20}$$

2.4.1. Hybridization and trajectory between the 1-lump and n-solitons

To obtain the hybrid solutions composed of 1-lump solution and n-solitons, we first take $N=3$, $\gamma_1 = \gamma_2 = I\pi$ in Eq. (5) and let $k_1 \to 0, k_2 \to 0$, then f_3 can be expressed as follows:

$$f_3 = \theta_1\theta_2 + \Lambda_{12} + \Big((\theta_1 + C_{13})(\theta_2 + C_{23}) + \Lambda_{12}\Big)\mathrm{e}^{\zeta_3}. \tag{21}$$

By substituting Eq. (21) into Eq. (3), the hybrid solution between 1-lump and 1-soliton is obtained. Via similar calculation, when $N=4$, we have

$$\begin{aligned} f_4 \;=\; & \theta_1\theta_2 + \Lambda_{12} + \big((\theta_1 + C_{13})(\theta_2 + C_{23}) + \Lambda_{12}\big)\mathrm{e}^{\zeta_3} \\ & + \big((\vartheta_1 + C_{14})(\theta_2 + C_{24}) + \Lambda_{12}\big)\mathrm{e}^{\zeta_4} \\ & + \big((\theta_1 + C_{13} + C_{14})(\theta_2 + C_{23} + C_{24}) + \Lambda_{12}\big) \\ & \times \mathrm{e}^{\zeta_3+\zeta_4}\exp(A_{34}). \end{aligned} \tag{22}$$

In Eqs. (21) and (22), the parameters satisfy the following relationship:

$$\begin{cases} \theta_i = m_i x - \dfrac{\beta m_i q_i + 3u_0 m_i^2 + q_i^2}{\alpha q_i} y + q_i t, & (i=1,2), \\ \zeta_j = k_j\Big(m_j x - \dfrac{k_j^2 m_j^3 q_3 + \beta m_j q_j + 3u_0 m_j^2 + q_j^2}{\alpha q_j} y + q_j t\Big) + \gamma_j, & (j=3,4), \\ \Lambda_{12} = \dfrac{2m_1 m_2 q_1 q_2 (m_1 q_2 + m_2 q_1)}{u_0 (m_1 q_2 - m_2 q_1)^2}, & \\ c_{ij} = -\dfrac{2k_j m_i m_j q_i q_j (m_i q_j + m_j q_i)}{k_j^2 m_i m_j^2 q_i q_j^2 - u_0 (m_i q_j - m_j q_i)^2}, & (i=1,2, j=3,4). \end{cases} \tag{23}$$

Similar to the cases of $N=3$ and $N=4$, we can obtain a general formula for the hybrid solutions between 1-lump and n-solitons,

$$f_{2+n} = \sum_{\mu=0,1} \left(\left(\theta_1 + \sum_{2\le r}^{2+n} \mu_r C_{1r}\right)\left(\theta_2 + \sum_{2\le l}^{2+n} \mu_l C_{2l}\right) + \Lambda_{12} \right) \exp\left(\sum_{i=2}^{2+n} \mu_i \zeta_i + \sum_{2\le i<j}^{2+n} \mu_i \mu_j A_{ij} \right), \tag{24}$$

where $\mu_2 = 0$, n is a positive integer, θ_i, ζ_j, Λ_{12} and c_{ij} satisfy Eq. (23). By substituting Eq. (24) into Eq. (3), we can obtain the hybrid solutions between 1-lump and n-solitons in Ito Eq. (1), also known as the interaction solutions between 1-lump and n-solitons. Next, we will provide the trajectory theorem of the 1-lump solution before and after interaction with n-solitons.

Theorem 1 On the condition of expression (24) and

$$\begin{aligned} \Omega_i \;=\; & \frac{k_i^3 m_i^3 q_1 q_2}{3u_0 m_1 m_2 - q_1 q_2} \\ & + \frac{3u_0 k_i (m_1 q_i + m_i q_1)(m_2 q_i + m_i q_2)}{q_i (3u_0 m_1 m_2 - q_1 q_2)}, \end{aligned} \tag{25}$$

the motion trajectory equations of the lump solution before and after interaction with n-soliton are

$$\begin{aligned} x_- \;=\; & -\frac{\beta q_1 q_2 + 3u_0(m_1 q_2 + m_2 q_1)}{3u_0 m_1 m_2 - q_1 q_2} t + \sum_{i=3}^{2+n} h_-(\Omega_i) D_i, \\ y_- \;=\; & -\frac{\alpha q_1 q_2}{3u_0 m_1 m_2 - q_1 q_2} t + \sum_{i=3}^{2+n} h_-(\Omega_i) E_i, \\ x_+ \;=\; & -\frac{\beta q_1 q_2 + 3u_0(m_1 q_2 + m_2 q_1)}{3u_0 m_1 m_2 - q_1 q_2} t + \sum_{i=3}^{2+n} h_+(\Omega_i) D_i, \\ y_+ \;=\; & -\frac{\alpha q_1 q_2}{3u_0 m_1 m_2 - q_1 q_2} t + \sum_{i=3}^{2+n} h_+(\Omega_i) E_i, \end{aligned} \tag{26}$$

where

$$\begin{aligned} D_i &= \frac{\varpi_2 q_1 C_{1i} - \varpi_1 q_2 C_{2i}}{3u_0 m_1 m_2 - q_1 q_2}, \\ E_i &= \frac{(m_2 C_{1i} - m_1 C_{2i})\,\alpha q_1 q_2}{(3u_0 m_1 m_2 - q_1 q_2)(m_1 q_2 - m_2 q_1)}, \\ \varpi_i &= \beta m_i q_i + 3u_0 m_i^2 + q_i^2, \quad (i=1,2), \end{aligned} \tag{27}$$

$$h_-(\Omega_i) = \begin{cases} 1, & \Omega_i < 0, \\ 0, & \Omega_i \ge 0, \end{cases} \quad h_+(\Omega_i) = \begin{cases} 1, & \Omega_i > 0, \\ 0, & \Omega_i \le 0. \end{cases} \tag{28}$$

In Eq. (26), (x_-, y_-) and (x_+, y_+) represent the trajectories before and after the collision, respectively.

Proof According to the analysis of the trajectory equation for 1-lump solutions in Subsection 2.3, we assume that the trajectory equations of the 1-lump solution before and after interaction with n-soliton are

$$\begin{aligned} x &= -\frac{\beta q_1 q_2 + 3u_0(m_1 q_2 + m_2 q_1)}{3u_0 m_1 m_2 - q_1 q_2} t + g_1, \\ y &= -\frac{\alpha q_1 q_2}{3u_0 m_1 m_2 - q_1 q_2} t + g_2. \end{aligned} \tag{29}$$

When $n=1$, substituting Eq. (29) into Eq. (21), f_3 can be

expressed as follows:

$$f_3 = \vartheta_1\vartheta_2 + \Lambda_{12} + ((\vartheta_1 + C_{13})(\vartheta_2 + C_{23}) + \Lambda_{12})\mathrm{e}^{\Omega_3 t+\sigma_3}, \quad (30)$$

with

$$\begin{aligned} \vartheta_i &= m_i g_1 + p_i g_2, \ \ (i = 1,2), \\ \sigma_i &= k_i m_i g_1 + k_i p_i g_2 + \gamma_i, \ \ (i = 1,2,\ldots,n). \end{aligned} \quad (31)$$

There are two cases $\Omega_3 > 0$ and $\Omega_3 < 0$ that need to be discussed, and since the calculation process for $\Omega_3 < 0$ is the same as $\Omega_3 > 0$, we will only discuss the case of $\Omega_3 > 0$ here. When t tends to positive and negative infinity, we can get the following approximate expressions of Eq. (30):

$$\begin{aligned} f_- &= \vartheta_1\vartheta_2 + \Lambda_{12}, \\ f_+ &= (\vartheta_1 + C_{13})(\vartheta_2 + C_{23}) + \Lambda_{12}. \end{aligned} \quad (32)$$

By substituting g_1 and g_2 in Eq. (29) into Eq. (32), we get

$$\begin{aligned} f_- &= \theta_1\theta_2 + \Lambda_{12}, \\ f_+ &= (\theta_1 + C_{13})(\theta_2 + C_{23}) + \Lambda_{12}. \end{aligned} \quad (33)$$

Similar to the method of finding the trajectory of 1-lump, we can get the following motion trajectory of the 1-lump solution before and after interaction with 1-soliton:

$$\begin{aligned} x_- &= -\frac{\beta q_1 q_2 + 3u_0(m_1 q_2 + m_2 q_1)}{3u_0 m_1 m_2 - q_1 q_2} t, \\ y_- &= -\frac{\alpha q_1 q_2}{3u_0 m_1 m_2 - q_1 q_2} t, \\ x_+ &= -\frac{\beta q_1 q_2 + 3u_0(m_1 q_2 + m_2 q_1)}{3u_0 m_1 m_2 - q_1 q_2} t \\ &\quad + \frac{\varpi_2 q_1 C_{13} - \varpi_1 q_2 C_{23}}{3u_0 m_1 m_2 - q_1 q_2}, \\ y_+ &= -\frac{\alpha q_1 q_2}{3u_0 m_1 m_2 - q_1 q_2} t \\ &\quad + \frac{(m_2 C_{13} - m_1 C_{23})\alpha q_1 q_2}{(3u_0 m_1 m_2 - q_1 q_2)(m_1 q_2 - m_2 q_1)}. \end{aligned} \quad (34)$$

When $n = 2$, similar to the calculation process for $n = 1$, we can get

$$\begin{aligned} f_4 &= \vartheta_1\vartheta_2 + \Lambda_{12} + [(\vartheta_1 + C_{13})(\vartheta_2 + C_{23}) + \Lambda_{12}]\mathrm{e}^{\Omega_3 t+\sigma_3} \\ &\quad + [(\vartheta_1 + C_{14})(\vartheta_2 + C_{24}) + \Lambda_{12}]\mathrm{e}^{\Omega_4 t+\sigma_4} \\ &\quad + [(\vartheta_1 + C_{13} + C_{14})(\vartheta_2 + C_{23} + C_{24}) + \Lambda_{12}] \\ &\quad \times \mathrm{e}^{\Omega_3 t+\sigma_3+\Omega_4 t+\sigma_4}\exp(A_{34}), \end{aligned} \quad (35)$$

In the following, we will discuss the two cases of $\Omega_3 > 0$, $\Omega_4 > 0$ and $\Omega_3 > 0$, $\Omega_4 < 0$, because other cases are similar to these two cases, so we will not discuss more. When $\Omega_3 > 0$, $\Omega_4 > 0$, similar to Eqs. (30)–(33), we can get the following approximate expressions of Eq. (23):

$$\begin{aligned} f_- &= \theta_1\theta_2 + \Lambda_{12}, \\ f_+ &= (\theta_1 + C_{13} + C_{14})(\theta_2 + C_{23} + C_{24}) + \Lambda_{12}. \end{aligned} \quad (36)$$

Similar to the calculation for $n = 1$, we can obtain the following motion trajectory of the 1-lump solution before and after interaction with 2-soliton:

$$\begin{aligned} x_- &= -\frac{\beta q_1 q_2 + 3u_0(m_1 q_2 + m_2 q_1)}{3u_0 m_1 m_2 - q_1 q_2} t, \\ y_- &= -\frac{\alpha q_1 q_2}{3u_0 m_1 m_2 - q_1 q_2} t, \\ x_+ &= -\frac{\beta q_1 q_2 + 3u_0(m_1 q_2 + m_2 q_1)}{3u_0 m_1 m_2 - q_1 q_2} t \\ &\quad + \frac{\varpi_2 q_1 (C_{13} + C_{14}) - \varpi_1 q_2 (C_{23} + C_{24})}{3u_0 m_1 m_2 - q_1 q_2}, \\ y_+ &= -\frac{\alpha q_1 q_2}{3u_0 m_1 m_2 - q_1 q_2} t \\ &\quad + \frac{\big(m_2(C_{13} + C_{14}) - m_1(C_{23} + C_{24})\big)\alpha q_1 q_2}{(3u_0 m_1 m_2 - q_1 q_2)(m_1 q_2 - m_2 q_1)}. \end{aligned} \quad (37)$$

When $\Omega_3 > 0$, $\Omega_4 < 0$, similar to Eqs. (30)–(33), we can get the following approximate expressions of Eq. (23):

$$\begin{aligned} f_- &= (\theta_1 + C_{14})(\theta_2 + C_{24}) + \Lambda_{12}, \\ f_+ &= (\theta_1 + C_{13})(\theta_2 + C_{23}) + \Lambda_{12}. \end{aligned} \quad (38)$$

Similar to Eq. (37), we can obtain the following motion trajectory for the 1-lump before and after the interaction:

$$\begin{aligned} x_- &= -\frac{\beta q_1 q_2 + 3u_0(m_1 q_2 + m_2 q_1)}{3u_0 m_1 m_2 - q_1 q_2} t \\ &\quad + \frac{\varpi_2 q_1 C_{14} - \varpi_1 q_2 C_{24}}{3u_0 m_1 m_2 - q_1 q_2}, \\ y_- &= -\frac{\alpha q_1 q_2}{3u_0 m_1 m_2 - q_1 q_2} t \\ &\quad + \frac{\big(m_2 C_{14} - m_1 C_{24}\big)\alpha q_1 q_2}{(3u_0 m_1 m_2 - q_1 q_2)(m_1 q_2 - m_2 q_1)}, \\ x_+ &= -\frac{\beta q_1 q_2 + 3u_0(m_1 q_2 + m_2 q_1)}{3u_0 m_1 m_2 - q_1 q_2} t \\ &\quad + \frac{\varpi_2 q_1 C_{13} - \varpi_1 q_2 C_{23}}{3u_0 m_1 m_2 - q_1 q_2}, \\ y_+ &= -\frac{\alpha q_1 q_2}{3u_0 m_1 m_2 - q_1 q_2} t \\ &\quad + \frac{\big(m_2 C_{13} - m_1 C_{23}\big)\alpha q_1 q_2}{(3u_0 m_1 m_2 - q_1 q_2)(m_1 q_2 - m_2 q_1)}. \end{aligned} \quad (39)$$

When $n \geq 3$ is any positive integer, similar to the calculation of $n = 1, 2$, we can get the following approximate expressions of Eq. (24):

$$\begin{aligned} f_- &= \sum_{\mu=0,1} \Bigg((\theta_1 + \sum_{i\neq r,l,\ldots,m,n}^{2+n} \mu_i C_{1i})(\theta_2 \\ &\qquad \sum_{j\neq r,l,\ldots,m,n}^{2+n} \mu_j C_{2j}) + \Lambda_{12} \Bigg), \\ f_+ &= \sum_{\mu=0,1} \Bigg((\theta_1 + \sum_{i=r,l,\ldots,m,n}^{2+n} \mu_i C_{1i})(\theta_2 \\ &\qquad + \sum_{j=r,l,\ldots,m,n}^{2+n} \mu_j C_{2j}) + \Lambda_{12} \Bigg), \end{aligned} \quad (40)$$

where $\Omega_r, \Omega_l, \ldots, \Omega_m, \Omega_n$ are positive, and Ω_i $(i \neq r, l, \ldots, m, n)$ is negative. Based on the above analysis of $n = 1, 2$, through Eq. (40), the trajectory equations of the 1-lump before and after the interaction with n-solitons are

$$\begin{aligned} x_- &= -\frac{\beta q_1 q_2 + 3u_0(m_1 q_2 + m_2 q_1)}{3u_0 m_1 m_2 - q_1 q_2} t + \sum_{i \neq r,l,\ldots,m,n}^{2+n} D_i, \\ y_- &= -\frac{\alpha q_1 q_2}{3u_0 m_1 m_2 - q_1 q_2} t + \sum_{i \neq r,l,\ldots,m,n}^{2+n} E_i, \\ x_+ &= -\frac{\beta q_1 q_2 + 3u_0(m_1 q_2 + m_2 q_1)}{3u_0 m_1 m_2 - q_1 q_2} t + \sum_{i = r,l,\ldots,m,n}^{2+n} D_i, \\ y_+ &= -\frac{\alpha q_1 q_2}{3u_0 m_1 m_2 - q_1 q_2} t + \sum_{i = r,l,\ldots,m,n}^{2+n} E_i. \end{aligned} \tag{41}$$

The proof of theorem is complete. Further more, we get the following corollary from theorem 1.

Corollary 1 The trajectory equations of 1-lump in the (x, y) plane before and after interaction with n-soliton are

$$\begin{aligned} y_- &= \frac{\alpha q_1 q_2}{\beta q_1 q_2 + 3u_0 (m_1 q_2 - m_2 q_1)} \\ &\quad \times \left(x_- - \sum_{i=3}^{2+n} h_- (\Omega_i) D_i \right) + \sum_{i=3}^{2+n} h_- (\Omega_i) E_i, \\ y_+ &= \frac{\alpha q_1 q_2}{\beta q_1 q_2 + 3u_0 (m_1 q_2 - m_2 q_1)} \\ &\quad \times \left(x_+ - \sum_{i=3}^{2+n} h_+ (\Omega_i) D_i \right) + \sum_{i=3}^{2+n} h_+ (\Omega_i) E_i, \end{aligned} \tag{42}$$

where the values of D_i and E_i are the same as those in Eq. (27).

Next, we will illustrate the hybridization behavior and trajectory equations of 1-lump before and after interaction with n-solitons through two examples.

Firstly, we will take the interaction between 1-lump and 1-soliton as an example to illustrate. Substituting Eqs. (20), (21) and (23) into Eq. (3), we can get the hybrid solution composed of the 1-lump solution and the 1-soliton. When the values of parameters are $u_0 = -\frac{1}{2}$, $k_3 = -\frac{1}{2}$, $a_{11} = -3$, $b_{11} = 2$, $c_{11} = -\frac{1}{8}$, $d_{11} = 3$, $q_3 = \frac{1}{4}$, $m_3 = 1$, $\alpha = 2$, $\beta = 1$, $\gamma_3 = 0$, the spatial evolution plots of hybrid solution can be shown in Fig. 5. From Figs. 5(a)–5(c), we can observe the collision process of the interaction between 1-lump and 1-soliton as time t changes. Before and after the interaction with solitons, lumps' waveform and spatial structure remain unchanged. Therefore, the collision between 1-lump and 1-soliton is an elastic collision. By substituting these parameter values into Eq. (34), we obtain the motion trajectory equation of the lump solution during the interaction process, which is shown in Fig. 5(d).

Secondly, we study the interaction behavior between 1-lump and 2-solitons. Substituting Eqs. (20), (22) and (23) into Eq. (3), we get 2-order hybrid solutions which are composed of 1-lump solution and 2-solitons. In Figs. 6(a)–6(c), when the values of parameters are $u_0 = -\frac{1}{2}$, $k_3 = -\frac{1}{2}$, $k_4 = -\frac{1}{4}$, $a_{11} = 1$, $b_{11} = 1$, $c_{11} = -\frac{1}{2}$, $d_{11} = 1$, $q_3 = \frac{1}{4}$, $q_4 = 1$, $m_3 = 1$, $m_4 = 1$, $\alpha = 2$, $\beta = 1$, $\gamma_3 = 0$, $\gamma_4 = 0$, we can get the spatial structure evolution plots of 2-order hybrid solution with different time. Similarly, by substituting these parameter values into Eq. (39), we obtain the motion trajectory equations of the 1-lump solution during the interaction process, which is shown in Fig. 6(d).

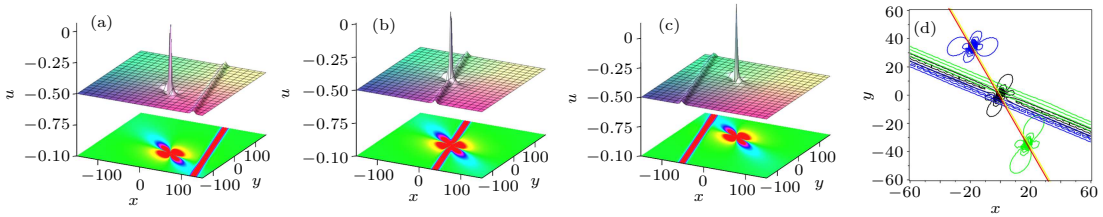


Fig. 5. The spatial evolution plots of hybrid behavior between 1-order lump solution and 1-soliton over time t: (a) $t = -40$, (b) $t = 0$, (c) $t = 40$. (d) The trajectory of u along $y_+ = -\frac{1154}{623} x_+ - \frac{91222546}{43251775}$ (red) and $y_- = -\frac{1154}{623} x_-$ (yellow) when $t = -40$ (green), 0 (black), 40 (blue).

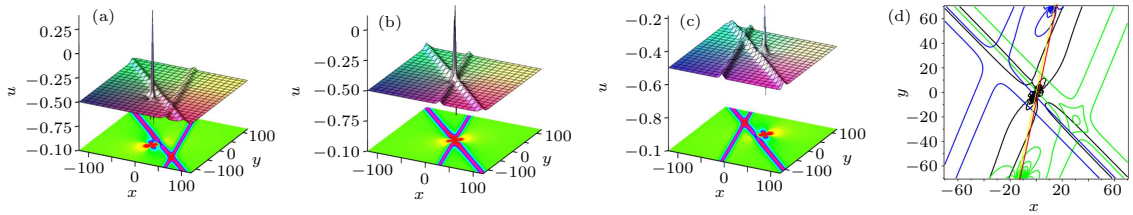


Fig. 6. The spatial evolution plots of hybrid behavior between 1-order lump solution and 2-soliton over time t: (a) $t = -40$, (b) $t = 0$, (c) $t = 40$. (d) The trajectory of u along $y_+ = 5x_+ - \frac{31352800}{23464657}$ (red) and $y_- = 5x_-$ (yellow) when $t = -40$ (green), 0 (black), 40 (blue).

2.4.2. Hybridization behavior between the 1-order breather wave and n-soliton ($n = 1, 2$)

In this subsection, the hybridization behavior between 1-breather wave and n-soliton $(n = 1, 2)$ is taken as an example to demonstrate the interaction behavior between breather waves and solitons. In order to get the hybridization behavior between 1-breather wave and and 1-soliton, we take $N = 3$ in Eq. (5), and then substitute it and Eq. (20) into Eq. (3). Fur-

thermore, the spatial structure diagrams of the hybridization between 1-breather wave and and 1-soliton can be obtained when the parameters are $a_{11}=0$, $b_{11}=\frac{1}{2}$, $c_{11}=-\frac{4}{5}$, $d_{11}=1$, $m_3=1$, $q_3=\frac{1}{2}$, $u_0=-\frac{1}{2}$, $\alpha=2$, $\beta=1$, $k_1=k_2=1$, $k_3=\frac{1}{2}$, $\gamma_i=0$ $(i=1,2,3)$.

When $N=4$, we can also get the hybridization behavior between 1-breather wave and and 2-solitons through the above method, and Fig. 8 can be obtained, when the parameters are $a_{11}=1$, $b_{11}=\frac{1}{4}$, $c_{11}=\frac{1}{12}$, $d_{11}=1$, $m_3=m_4=2$, $q_3=1$, $q_4=\frac{1}{2}$, $u_0=-\frac{1}{2}$, $\alpha=2$, $\beta=1$, $k_i=\frac{1}{2}$, $\gamma_i=0$ $(i=1,\ldots,4)$.

Due to the complexity of the expression for hybrid solutions between breather waves and n-solitons $(n=1,2)$, we only provide the spatial structural evolution diagrams of the hybrid behavior over time t here. The structural changes in the interaction process between breather waves and n-solitons $(n=1,2)$ can be clearly observed from Figs. 7 and 8, respectively. The trajectory equations, motion velocity, interaction deformation, and other dynamic properties of the interaction between breather waves and n-solitons will be the focus of our future research.

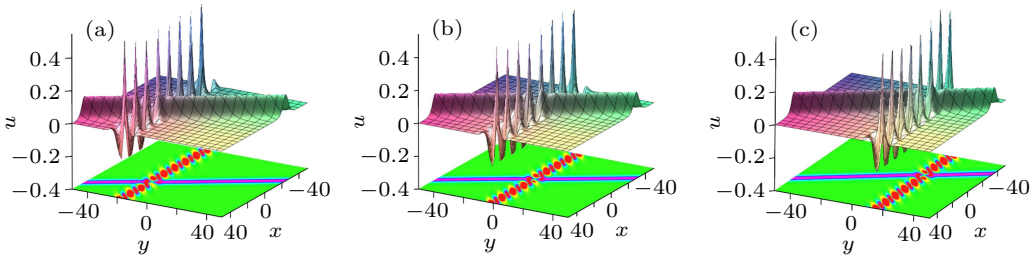


Fig. 7. The spatial evolution plots of hybrid behavior between 1-order breather wave and 1-soliton over time t: (a) $t=-10$, (b) $t=0$, (c) $t=10$.

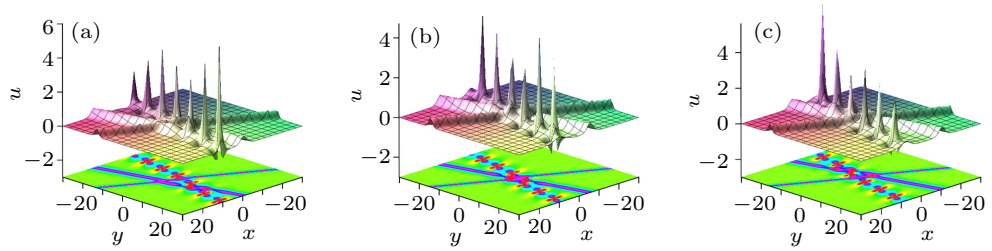


Fig. 8. The spatial evolution plots of hybrid behavior between 1-order breather wave and 2-soliton over time t: (a) $t=-10$, (b) $t=0$, (c) $t=10$.

3. The novel multi-solitons and lump solutions

Seeking new soliton solutions and studying the structural properties of solitons have always been a hot research topic in the field of solitons and integrable systems. In this section, based on the three-wave solution, breather wave, rogue wave and lump solution of the Ito Eq. (1),[24] we choose a new test function to study the multi-solitons and new lump solutions of the Ito Eq. (1). Here, to expand the research results of Refs. [23,30], let $u_0=0$ in bilinear Eq. (4). We construct the following test functions:

$$\begin{aligned} f(x,y,t) &= b_1\cosh(\delta_1)+b_2\cos(\delta_2) \\ &\quad +b_3\cosh(\delta_3)+b_4\cos(\delta_4), \end{aligned} \tag{43}$$

where $\delta_i=k_i(a_ix+p_iy+q_it+\gamma_i)$ $(i=1,2\ldots,4)$, and k_i,a_i,p_i,q_i,γ_i are free parameters that will be determined. Substituting Eq. (43) into Eq. (4) and combining with Maple 2022, we get the following set of parameter relations:

$$\begin{aligned} &a_1=\frac{k_3a_3}{k_1},\quad a_2=-\frac{k_4a_4}{k_2}, \\ &p_1=-\frac{q_1}{\alpha}-\frac{\sigma}{\alpha k_1},\quad p_2=\frac{k_4a_4(3k_3^2a_3^2-k_4^2a_4^2+\beta)-\chi}{\alpha k_2}, \\ &p_3=\frac{k_1q_1}{\alpha k_3}-\frac{\sigma}{\alpha k_3},\quad p_4=-\frac{k_4a_4(3k_3^2a_3^2-k_4^2a_4^2+\beta)+\chi}{\alpha k_4}, \\ &q_2=\frac{\chi}{k_2},\quad q_3=-\frac{k_1q_1}{k_3},\quad q_4=\frac{\chi}{k_4}, \end{aligned} \tag{44}$$

where

$$\chi=\frac{k_1k_3a_3q_1(b_1^2-b_3^2)}{k_4a_4(b_2^2-b_4^2)},\quad \sigma=k_3a_3(k_3^2a_3^2-3k_4^2a_4^2+\beta).$$

Substituting Eqs. (43) and (44) into Eq. (3), we obtain the following multi-breather solution:

$$\begin{aligned} u &= 2\Bigg(\frac{b_1k_1^2a_1^2\cosh\delta_1-b_2k_2^2a_2^2\cos\delta_2+b_3k_3^2a_3^2\cosh\delta_3-b_4k_4^2a_4^2\cos\delta_4}{b_1\cosh\delta_1+b_2\cos\delta_2+b_3\cosh\delta_3+b_4\cos\delta_4} \\ &\quad -\frac{(b_1k_1a_1\sinh\delta_1-b_2k_2a_2\sin\delta_2+b_3k_3a_3\sinh\delta_3-b_4k_4a_4\sin\delta_4)^2}{(b_1\cosh\delta_1+b_2\cos\delta_2+b_3\cosh\delta_3+b_4\cos\delta_4)^2}\Bigg), \end{aligned} \tag{45}$$

$$
\begin{aligned}
v \;=\; & u_0+2\left(\frac{b_1k_1^2a_1q_1\cosh\delta_1-b_2k_2^2a_2q_2\cos\delta_2+b_3k_3^2a_3q_3\cosh\delta_3-b_4k_4^2a_4q_4\cos\delta_4}{b_1\cosh\delta_1+b_2\cos\delta_2+b_3\cosh\delta_3+b_4\cos\delta_4}\right)\\
& -2\left(\frac{b_1k_1a_1\sinh\delta_1-b_2k_2a_2\sin\delta_2+b_3k_3a_3\sinh\delta_3-b_4k_4a_4\sin\delta_4}{b_1\cosh\delta_1+b_2\cos\delta_2+b_3\cosh\delta_3+b_4\cos\delta_4}\right.\\
& \left.\times\frac{b_1k_1q_1\sinh\delta_1-b_2k_2q_2\sin\delta_2+b_3k_3q_3\sinh\delta_3-b_4k_4q_4\sin\delta_4}{b_1\cosh\delta_1+b_2\cos\delta_2+b_3\cosh\delta_3+b_4\cos\delta_4}\right).
\end{aligned}
\tag{46}
$$

In fact, the multi-soliton given by expression (45) is a multi-breather solution that exhibits periodic characteristics on variables δ_2 or δ_4, while having soliton characteristics on variables δ_1 or δ_3. The multi-breather solution (45) obtained here is different from the higher-order breather solution in Subsection 2.2, which is a new soliton solution. When $b_3=0$ and $b_4=0$ (or $b_1=0$ and $b_2=0$), the solution (45) is simplified as 1-order breather wave solution (see Fig. 9(a)),[30] we obtain a new 1-order breather wave solution, which has a different structure from the breather wave (10). From Fig. 9(a), it can be observed that its spatial structure has a kink property, also known as the kinky breather wave solution.[37] When $b_4=0$ (or $b_2=0$), solution (45) is simplified as a double-breather solitary solution (see Fig. 9(b)).[23,38] Meanwhile, due to the periodicity of $\cos\delta_2$ and $\cos\delta_4$ function, the solution (45) shows the characteristics of local oscillation. Therefore, analytical solutions with this characteristic can also be called multi-breather solutions (see Fig. 9(c)), which have characteristics different from high-order breather solutions. In order to better show the deformation behavior of multi-breather solution, we present a spatiotemporal structure diagram in Fig. 9, where the same parameter values are $u_0=1$, $a_3=2$, $a_4=1$, $q_1=1$, $\alpha=2$, $\beta=1$, $k_1=k_2=k_4=1$, $k_3=\frac{1}{2}$, $\gamma_i=0$ $(i=1,\ldots,4)$, while different parameter values are (a) $b_1=3$, $b_2=1$, $b_3=b_4=0$, $k_3=\frac{1}{3}$, (b) $b_1=-3$, $b_2=0$, $b_3=-2$, $b_4=4$ and (c) $b_1=3$, $b_2=1$, $b_3=2$, $b_4=4$.

To construct the lump solutions, we choose $k_2=rk_1$, $k_3=sk_1$, $k_4=lk_1$, $b_1=\cosh(mk_1)$, $b_2=-\cos(nk_1)$, $b_3=\cos(hk_1)$, $b_4=-\cosh(gk_1)$ in Eq. (45), and the parameters r, s, l, m, n, h, g can take any pure imaginary number and real number. Letting $k_1\to 0$, we get

$$
\begin{aligned}
u \;=\; & 2\left(\frac{2s^2a_3^2+2l^2a_4^2}{\frac{1}{2}\Omega_1^2+\frac{1}{2}r^2\Omega_2^2+\frac{1}{2}\Omega_3^2+\frac{1}{2}l^2\Omega_4^2+\frac{1}{2}(m^2+n^2-h^2-g^2)}-\frac{(sa_3\Omega_1-lra_4\Omega_2+sa_3\Omega_3+l^2a_4\Omega_4)^2}{(\frac{1}{2}\Omega_1^2+\frac{1}{2}r^2\Omega_2^2+\frac{1}{2}\Omega_3^2+\frac{1}{2}l^2\Omega_4^2+\frac{1}{2}(m^2+n^2-h^2-g^2))^2}\right),\\
v \;=\; & u_0+2\left(\frac{(sa_3\Omega_1-lra_4\Omega_2+sa_3\Omega_3+l^2a_4\Omega_4)}{\frac{1}{2}\Omega_1^2+\frac{1}{2}r^2\Omega_2^2+\frac{1}{2}\Omega_3^2+\frac{1}{2}l^2\Omega_4^2+\frac{1}{2}(m^2+n^2-h^2-g^2)}\frac{(q_1\Omega_1-\frac{a_3q_1sr(h^2+m^2)}{la_4(n^2+g^2)}\Omega_2-q_1\Omega_3-\frac{a_3q_1s(h^2+m^2)}{a_4(n^2+g^2)}\Omega_4)}{\frac{1}{2}\Omega_1^2+\frac{1}{2}r^2\Omega_2^2+\frac{1}{2}\Omega_3^2+\frac{1}{2}l^2\Omega_4^2+\frac{1}{2}(m^2+n^2-h^2-g^2)}\right),
\end{aligned}
\tag{47}
$$

where $\Omega_i=\lim\limits_{k_1\to 0}\delta_i/k_1$ $(i=1,\ldots,4)$, that is

$$
\begin{aligned}
\Omega_1 \;=\; & sa_3x-\frac{(\beta sa_3+q_1)}{\alpha}y+q_1t+\gamma_1,\\
\Omega_2 \;=\; & -\frac{la_4}{r}x+\frac{sa_3q_1(m^2+h^2)+\beta l^2a_4^2(n^2+g^2)}{\alpha lra_4(n^2+g^2)}y\\
& -\frac{sa_3q_1(h^2+m^2)}{lra_4(n^2+g^2)}t+\gamma_2,\\
\Omega_3 \;=\; & sa_3x-\frac{(\beta sa_3-q_1)}{\alpha}y-q_1t+s\gamma_3,\\
\Omega_4 \;=\; & a_4x+\frac{sa_3q_1(h^2+m^2)-\beta l^2a_4^2(n^2+g^2)}{\alpha l^2a_4(n^2+g^2)}y\\
& -\frac{sa_3q_1(h^2+m^2)}{l^2a_4(n^2+g^2)}t+\gamma_4.
\end{aligned}
\tag{48}
$$

The solution represented by expression (48) is a lump solution, and from the analytical expressions of functions u and v, it can be concluded that there is no nonsingular when $m^2+n^2-h^2-g^2>0$, and also has the property of $(u,v)\to(0,u_0)$ when $\sqrt{x^2+y^2+t^2}\to\infty$. Here, we give the spatial structure of lump solution u and v, with the values of parameters as $u_0=1$, $a_3=1$, $a_4=2$, $q_1=2$, $g=2$, $n=1$, $h=\frac{1}{2}$, $m=\frac{1}{4}$, $l=\frac{1}{4}$, $s=2$, $r=-1$, $\alpha=\frac{1}{2}$, $\beta=0$, $\gamma_i=0$ $(i=1,\ldots,4)$ (see Fig. 9(d)).

Actually, based on Refs. [23,24,30,38,39] and the above research, we conclude that the (2+1)-dimensional Ito Eq. (1)) has the following form of multi-solitons, further, a new lump solution can be obtained according to the parameter limit method. Therefore, we construct the following test function:

$$
\begin{aligned}
f(x,y,t) \;=\; & \sum_{i=1}^{N}b_i\cosh\left(k_i(a_ix+p_iy+q_it+\gamma_i)\right)\\
& +\sum_{j=1}^{M}m_j\cos\left(l_j(c_jx+h_jy+g_jt+r_j)\right),
\end{aligned}
\tag{49}
$$

where b_i, k_i, a_i, p_i, q_i, γ_i $(i=1,2\ldots,N)$, m_j, l_j, c_j, h_j, g_j, r_j $(j=1,2\ldots,M)$ represents any constant, N and M can take any positive integer. However, due to the large number of parameters and computational complexity, this will be our future research focus on the (2+1)-dimensional Ito Eq. (1).

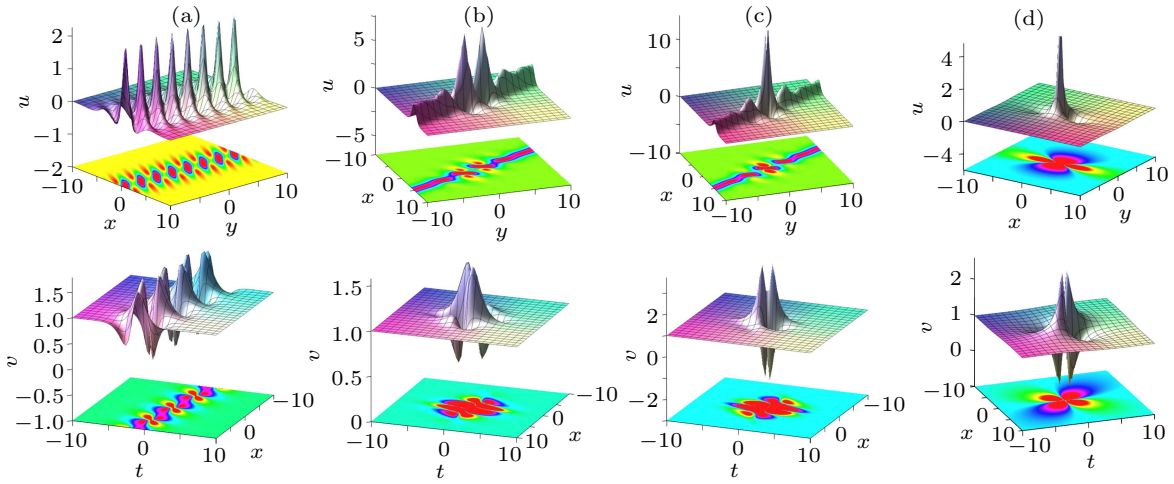


Fig. 9. The spatial evolution plots of multi-solitons Eq. (45), (a) 1-order breather solution; (b) double breather solution; (c) multi-breather solution. (d) The spatial structure plots of lump solution (47).

4. Conclusions

In this work, the equivalent coupled system of (2+1)-dimensional Ito's equation is introduced and a new bilinear equation is constructed. Based on the bilinear equation, some new multi-soliton solutions and hybrid behavior with lump solutions are investigated. On the basis of N-soliton solutions, the high-order breather waves can be obtained by the paired-complexification of parameters. We get the N-order rational solutions from N-soliton solutions, and then get the M-lump solutions from them by the paired-complexification of parameters. Moreover, we analyze the trajectory of M-lump solutions and provide their trajectory diagrams. Besides, appropriate parameters are selected to construct three-dimensional diagrams to show the hybridization behavior between lump solutions, breather waves and n-solitons ($n = 1, 2$), and the trajectory theorem of 1-lump before and after interaction with solitons are given and proved. Finally, we obtain some new lump solutions from the breather-wave solutions by constructing a new test function and using the parameter limit method. The trajectory equation, motion velocity, collision deformation and other dynamic properties of high-order lump solutions, the interaction behavior between breathers and n-solitons, as well as the breather solutions and evolutionary behavior in the form of test function (49), are all issues worth further research in our future work.

Acknowledgements

Project supported by the National Natural Science Foundation of China (Grant No. 12461047) and the Scientific Research Project of the Hunan Education Department (Grant No. 24B0478).

References

[1] Si Z Z, Wang Y Y and Dai C Q 2024 *Sci. China Phys. Mech.* **67** 1
[2] Si Z Z, Wang D L, Zhu B W, Ju Z T, Wang X P, Liu W, Malomed B A, Wang Y Y and Dai C Q 2024 *Laser Photonics Rev.* **18** 2400097
[3] Ju Z T, Si Z Z, Xin Y and Dai C Q 2024 *Chin. Phys. Lett.* **41** 084203
[4] Ablowitz M J and Clarkon P A 1991 *Solitons, Nonlinear Evolution and Inverse Scattering* (Cambridge: Cambridge University Press)
[5] Hirota R and Satsuma J 1981 *Phys. Lett. A* **85** 407
[6] Hirota R 2004 *The Direct Method in Soliton Theory* (Cambridge: Cambridge University Press)
[7] Gu C H, Hu H S and Zhou Z X 1999 *Darboux Transformation in Soliton Theory and Geometric Applications* (Shanghai: Shanghai Science and Technology Press)
[8] Matveev V B and Salle M A 1991 *Darboux Transformation and Solitons* (Springer: Springer series in nonlinear dynamics)
[9] Its A 2003 *Notices of the AMS* **50** 1389
[10] Wang D S and Wang X 2018 *Nonlinear Anal. Real World Appl.* **41** 334
[11] Ma Y L, Wazwaz A M and Li B Q 2023 *Phys. Lett. A* **488** 129132
[12] Feng B F, Ling L M and Takahashi D 2020 *Stud. Appl. Math.* **142** 46
[13] Chen S J, Yin Y H and Lü X 2024 *Commun. Nonlinear Sci. Numer. Simulat.* **130** 107205
[14] Ma Y L, Wazwaz A M and Li B Q 2021 *Phys. Lett. A* **413** 127585
[15] Kai Y, Ji J L and Yin Z X 2022 *Phys. Lett. A* **421** 127780
[16] Yan X Y, Liu J Z and Xin X P 2023 *Chin. Phys. B* **32** 070201
[17] Xia Y R, Zhang K K, Yao R X and Shen Y L 2023 *Chin. Phys. B* **32** 100201
[18] Wang X M, Tan W and Huang J J 2024 *Phys. Scr.* **99** 045201
[19] Ito M 1980 *J. Phys. Soc. Jpn.* **49** 771
[20] Adem A R 2016 *Comput. Math. Appl.* **71** 1248
[21] Zhang X, Wang C and Zhou Y 2021 *Phys. Scr.* **96** 075215
[22] Wang X B, Tian S F and Qin C Y 2017 *Appl. Math. Lett.* **68** 40
[23] Tan W 2021 *Int. J. Comput. Math.* **98** 961
[24] Tian Y and Dai Z 2015 *Z. Naturforsch. A* **70** 437
[25] Yang J Y, Ma W X and Qin Z 2018 *Anal. Math. Phys.* **8** 427
[26] Zou L, Yu Z B and Tian S F 2018 *Mod. Phys. Lett. B* **32** 1850104
[27] Ma W X, Yong X and Zhang H Q 2018 *Comput. Math. Appl.* **75** 289
[28] Wazwaz A M 2022 *Nonlinear Dyn.* **109** 1929
[29] Ilyas M A and Javid A 2023 *Optik* **293** 171405
[30] Tan W, Dai Z D and Dai H P 2017 *Therm. Sci.* **21** 1673
[31] He C H, Tang Y N, Ma W X and Ma J L 2019 *Nonlinear Dyn.* **95** 29
[32] Gong Q K, Wang H and Wang Y H 2024 *Chin. Phys. B* **33** 040505
[33] Tan W, Dai Z D and Xie J L 2018 *Comput. Math. Appl.* **75** 4214
[34] Huang J J, Tan W and Wang X M 2023 *Phys. Scr.* **98** 045226
[35] Akhmediev N N and Korneev V I 1986 *Theor. Math. Phys.* **69** 1089
[36] Zhang Z, Yang X Y, Li W T and Li B 2019 *Chin. Phys. B* **28** 110201
[37] Tan W and Dai Z D 2016 *Nonlinear Dyn.* **85** 817
[38] Tan W 2019 *Phys. Lett. A* **383** 125907
[39] Tan W, Zhang W and Zhang J 2020 *Appl. Math. Lett.* **101** 106063